JOURNAL OF MATERIALS SCIENCE 29 (1994) 3577–3590

Abnormal grain growth in alumina-doped hafnia ceramics

J. WANG, C. B. PONTON, P. M. MARQUIS
IRC in Materials for High Performance Applications and School of Metallurgy and Materials and School of Dentistry, The University of Birmingham, Birmingham B15 2TT, UK

Hafnia (HfO_2) ceramics containing 0.0, 5.0, and 10.0 vol% Al_2O_3, respectively, were sintered at 1600 °C for various periods from 2–24 h. Abnormal grain growth was found to occur in the Al_2O_3-containing compositions. Hafnia containing 5.0 vol% Al_2O_3 exhibits an average grain size of almost double that of the Al_2O_3-free hafnia matrix, coupled with a much wider grain-size distribution. The material containing 10.0 vol% Al_2O_3 shows a smaller average grain size than the composition containing 5.0 vol% Al_2O_3. However, its average grain size is still larger than that of the Al_2O_3-free hafnia on sintering at 1600 °C for more than 8 h. Microstructural characterization, carried out using scanning electron microscopy (SEM) and transmission electron microscopy (TEM) equipped with an energy dispersive analysis facility (EDX), indicated that there existed a continuous segregant layer at the grain boundaries and grain junctions in the Al_2O_3-free hafnia. Hafnia exhibits a low solubility in the segregant layer phase which inhibits the growth of the hafnia grains. The Al_2O_3 particles act as a scavenger for the silicon-rich glassy phase, damaging the continuous nature of the boundary segregant layer and promoting grain growth in the Al_2O_3-doped hafnia ceramics. The microstructural development at the sintering temperature is an overall result of the concurrent scavenger effect and grain pinning by the Al_2O_3 particles.

1. Introduction

Following the discovery of transformation toughening in the late 1970s [1], a variety of hafnia-based and hafnia-containing ceramics has been developed, including partially and fully stabilized hafnias and hafnia-dispersed ceramic matrices such as Al_2O_3–HfO_2, Al_2O_3–Cr_2O_3–HfO_2–ZrO_2, SiC–HfO_2 and Si_3N_4–HfO_2 [2]. These hafnia-containing ceramics, similar to zirconia transformation toughened ceramics, demonstrate improved fracture strength and fracture toughness. Furthermore, they exhibit a better performance at elevated temperatures than their zirconia counterparts, as the temperature for the tetragonal to monoclinic transformation in the former is higher (1700 °C) than that in the latter (1050 °C) [3, 4]. An alloy of hafnia–zirconia solid solution with an appropriate composition offers desirable mechanical properties over both the intermediate- and high-temperature ranges. Ceramic matrices containing an appropriate amount of unstabilized hafnia have excellent thermal shock resistance, due to the presence of a well-established microcrack network formed as a result of the volume expansion and shear strain associated with the HfO_2 (tetragonal) to HfO_2 (monoclinic) transformation on cooling from the sintering temperature [5].

Unstabilized hafnia exhibits a monoclinic structure at temperatures below 1700 °C and a low degree of sinterability [2, 6, 7]. The poor microstructure of pressureless sintered hafnia ceramics is characterized by a high level of porosity and/or microcracks and a large grain growth coupled with a wide grain-size distribution. Microstructural refinement is therefore important in fabricating hafnia-based ceramics. Unfortunately, little work has been carried out on the microstructural control in these materials via mechanisms such as a second-phase addition. Microstructural refinement has, however, been observed in several ceramic systems when an appropriate amount of second-phase particles is introduced as a grain-growth inhibitor. The best known example is zirconia-dispersed alumina ceramics [8], where the grain growth of an alumina matrix is effectively under control as a result of the pinning effect of the zirconia grains to the alumina matrix. For the ionically conductive zirconia ceramics, stabilized with Y_2O_3, CaO or Yb_2O_3, the purpose of an appropriate alumina addition is more than single-fold [9, 10]: firstly, the alumina inclusions inhibit the grain growth of the zirconia matrix, resulting in an improvement in mechanical performance; secondly, they act as a scavenger for the silica and/or silicate impurity present at the grain boundaries and grain junctions of the zirconia matrix, leading to an increase in ionic conductivity.

It is considered that the same approach may be applied to hafnia-based ceramics, as hafnia and zirconia are almost identical in crystal structure and reactivity and they form continuous solid solution over the entire composition range [2]. Commercial sources of hafnium oxide and hafnium chemicals often

0022–2461

contain 2–3 mol% zirconium compound as an understood impurity. Ceramic-grade hafnia raw materials almost always contain a level of silica or silicate impurity, as they were originally processed from either hafnium-containing zirconium silicate (zircon: $ZrSiO_4$) or silica-contaminated baddeleyite (naturally occurring monoclinic zirconia) [11, 12]. Few investigations have been made of the exact effect of a trace amount of silica or silicate impurity on the grain growth and microstructural development of hafnia ceramics at the sintering temperature. A similar situation is probably true for zirconia-based ceramics, although it has been observed that a residual silica or silicate impurity results in the occurrence of a glassy grain-boundary phase and the formation of a rounded grain morphology [13, 14]. It has been suggested that the intergranular liquid phase, consisting of various silicates, inhibits the grain growth of zirconia ceramics at the sintering temperature [14–17]. Two approaches may be taken in order to eliminate the impurity effect of a trace amount of silica or silicate present in a sintered hafnia ceramic: (i) utilizing an ultra-pure starting material, which is technically difficult to obtain and is not economically cost-effective for a large-scale production; (ii) using an appropriate additive to offset the impurity effect of a trace amount of silica or silicate present in the as-received hafnia powder, as has been demonstrated in both ionically conductive zirconia and ceria-stabilized tetragonal zirconia polycrystals (Ce–TZP). The objective of the present work was two-fold: (a) to study the effect of a small alumina addition on the sintering and microstructural development of a commercially available hafnia powder which contains 0.1–0.2 wt % silica as the principal impurity; (b) to determine if the alumina particles act as a scavenger for the silica impurity in the ceramic-grade hafnia.

2. Experimental procedure

The unstabilized hafnia powder used for the present investigation was from a commercial source (H.C. Starch GmbH & Co KG, Germany). It was estimated, on the basis of microstructural study carried out using analytical TEM on sintered samples, that there existed 0.1–0.2 wt % silica in the as-received hafnia powder as the principal impurity. Aluminium nitrate (BDH, UK) was used for the source of alumina addition. Three compositions were prepared, containing 0.0, 5.0 and 10.0 vol % Al_2O_3 in hafnia, respectively. Appropriate amounts of the as-received hafnia powder and aluminium nitrate were mixed together by ball milling in propanol using zirconia balls as the milling medium for 12 h. The Al_2O_3-free composition was subjected to the identical ball-milling procedure in order to eliminate the large powder agglomerates. Each milled powder suspension was then dried using a combination of a hot plate and heating lamp, followed by a calcination at 600 °C for 5 h to decompose the aluminium nitrate. The calcined powders were further ball milled in propanol for 24 h and dried, prior to compaction in a steel die of 12.5 mm diameter at a pressure of 120 MPa. The resultant green density after compaction was 59% theoretical density. The powder compacts were then sintered in electric furnaces at 1600 °C for various periods from 2–24 h. The sintered density of each sintered compact was measured using the Archimedes method in distilled water.

X-ray diffraction (XRD) phase analysis (CuK_α) was used to identify the phases present in the as-sintered specimens. Each sintered ceramic compact was then polished to 1 μm finish using diamond pastes and thermally etched at 1400 °C for 15 min for revealing the grain boundaries. Scanning electron microscopy (Joel 5000) was employed to characterize both the fracture and polished and then etched surfaces. The average grain size and grain-size distribution of both the hafnia matrix and alumina inclusions were determined using an image analyser (Quantimet 500, Leica, Cambridge, UK) on the scanning electron micrographs, when more than 300 grains were counted for each measurement. For microstructural examination using TEM, slices 200 μm thick were cut using a diamond slicing wheel from the sintered ceramics. The slices were ground to approximately 100 μm thickness using a silicon carbide slurry (400 grit) and specimen discs of 3 mm diameter were then prepared. The discs were further polished and then dimpled using a dimpler (Model 515, South Bay Technology, CA). The dimpled discs were finally polished in an ion-beam thinner (Model 600, Gatan, UK) and coated with carbon prior to being examined using a transmission electron microscopy (Joel-4000CX) equipped with an energy dispersion analysis facility (EDX).

3. Results and discussion

The Al_2O_3-free hafnia exhibited a brown appearance on sintering at 1600 °C for 2 h and became slightly fainter with increasing sintering time from 2–24 h. The Al_2O_3-doped hafnias appeared yellowish white when sintered at 1600 °C. They consisted of monoclinic hafnia and α-alumina (for the alumina-doped), as indicated by XRD phase analysis. Cracks were not found on the sintered surfaces of either the Al_2O_3-free or the Al_2O_3-doped specimen compacts, although the sintered density decreases slightly with increasing sintering time at 1600 °C, as shown in Fig. 1. The

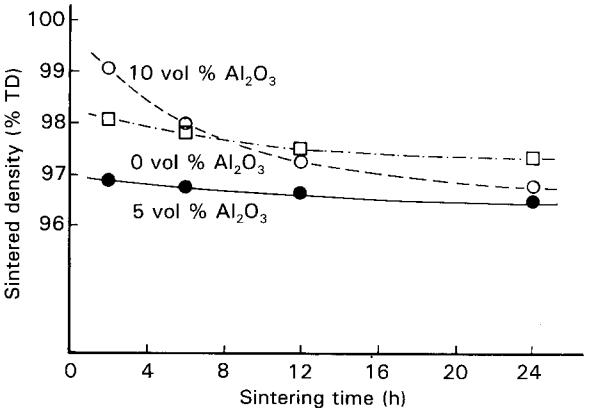

Figure 1 The sintered density as a function of sintering time at 1600 °C for hafnia ceramics containing 0, 5 and 10 vol % Al_2O_3, respectively.

hafnia ceramic containing 5.0 vol % Al_2O_3 is the lowest in sintered density, and that containing 10.0 vol % Al_2O_3 shows the largest decrease in the sintered density with increasing sintering time at 1600 °C. No phase transformation was involved when each powder compact was heated to and kept at 1600 °C, because the sintering temperature was below the monoclinic to tetragonal transformation temperature in hafnia [2, 3]. It is believed that the growth of the monoclinic hafnia grains is the dominant factor which contributes to the decrease in sintered density when the specimens are subjected to an extended duration at the sintering temperature. Another contributing factor to the decrease in the sintered density with increasing sintering time is the occurrence of residual strains induced by the anisotropic thermal contraction of the monoclinic hafnia grains on cooling from the sintering temperature [18, 19]. An increase in grain size will lead to an increase in the magnitude of the thermal strain energy in non-cubic polycrystalline ceramics [20]. The thermal strain energy may result in the formation of a network of microcracks at the grain boundaries, if it is above a critical value and not effectively accommodated by a plastically deformable grain-boundary phase. In many ceramic materials, the thermal strain is often accommodated, to a certain extent, by a glassy grain-boundary phase present as a result of silica/silicate impurity in the starting materials. As will be discussed below, abnormal grain growth occurred in the alumina-doped hafnia ceramics. Microstructural studies using TEM on more than 500 hafnia grains showed that the formation of microcracks at the grain boundaries were directly related to the grain sizes. Microcracks were not found in the area of small grain sizes and were observed to occur at the grain boundaries in the areas where there exists one or more large grains (> 5 μm) in the 5.0 vol % Al_2O_3-doped hafnia. Similarly, microstructural study carried out using SEM on the polished and then thermally etched surfaces revealed that the poor microstructure, represented by the presence of large pores and cracks, was often found in the regions where there existed one or more larger-than-average grains. Fig. 2 is a scanning electron micrograph showing the poor microstructure associated with abnormal grain growth in the 5.0 vol % Al_2O_3-doped hafnia, which was sintered at 1600 °C for 6 h.

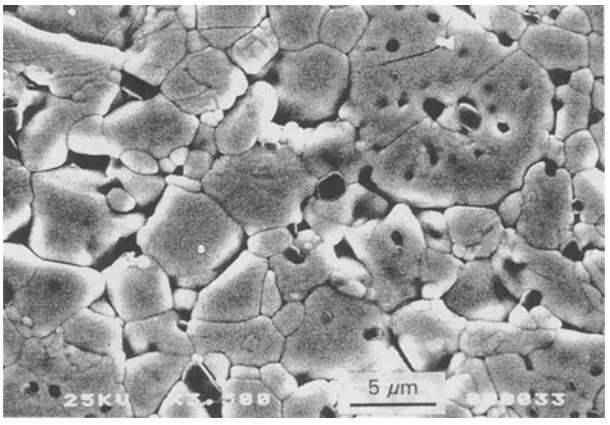

Figure 2 A scanning electron micrograph showing the poor microstructure in the region where abnormal grain growth occurs in the hafnia ceramic containing 5 vol % Al_2O_3, sintered at 1600 °C for 6 h.

Fig. 3 plots the average grain size of the hafnia matrix versus sintering time at 1600 °C for the three compositions containing 0.0, 5.0 and 10.0 vol % Al_2O_3, respectively. The Al_2O_3-free hafnia shows a steady increase in the average grain size when the sintering time increases from 2 h to 12 h and the increase slows down with a further increase in the sintering time above 12 h. The hafnia doped with 5.0 vol % Al_2O_3 exhibits the largest average grain size when sintered at 1600 °C. Its average gain size increases only slightly with increasing sintering time at the sintering temperature. The average grain size of the ceramic containing 10.0 vol % Al_2O_3 is slightly smaller than that of the undoped hafnia when sintered at 1600 °C for 2 h. However, it demonstrates the largest increase in average grain size with increasing sintering time at 1600 °C. In Fig. 4, the average grain size of the hafnia matrix is plotted against alumina

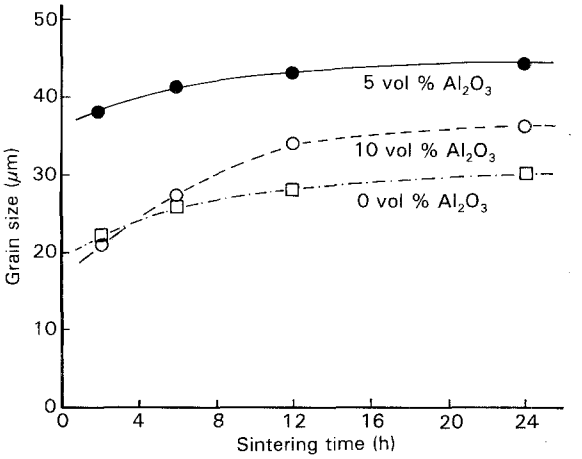

Figure 3 The average grain size of hafnia matrix as a function of sintering time at 1600 °C for the hafnia ceramics containing 0, 5 and 10 vol % Al_2O_3, respectively.

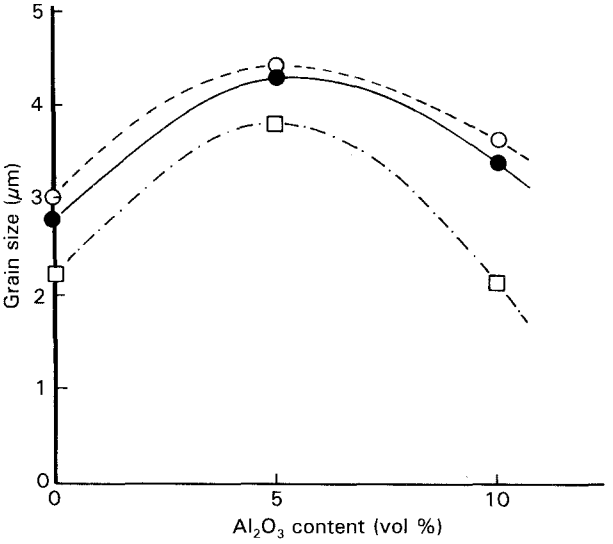

Figure 4 The average grain size of hafnia matrix as a function of alumina content (vol %) in the materials sintered at 1600 °C for (□) 2, (●) 12 and (○) 24 h, respectively.

content (vol %) for the materials sintered at 1600 °C for 2, 12 and 24 h, respectively. It demonstrates the fact that the maximum average grain size occurs in the composition containing 5.0 vol % Al_2O_3. To support further the experimental results shown in Figs 3 and 4, Figs 5a–c and 6a–c are scanning electron micrographs showing the polished and then thermally etched surfaces of the three compositions sintered at 1600 °C for 2 and 12 h, respectively. No significant abnormal grain growth is seen in the Al_2O_3-free hafnia on sintering at the sintering temperature for 2 h and a limited number of noticeably larger-than-average grains are found when sintered for 12 h. In contrast, the hafnia containing 5.0 vol % Al_2O_3 shows a typical microstructure of abnormal grain growth with many small alumina inclusions being entrapped within certain huge hafnia grains, although some large alumina particles are left at the grain boundaries and grain junctions of the hafnia matrix. The alumina inclusions, which are larger in size than those in the composition containing 5.0 vol % alumina, are present mainly at the grain boundaries and grain junctions of the hafnia matrix in the composition containing 10.0 vol % Al_2O_3. On sintering at 1600 °C for 2 h, abnormal grain growth is not substantial in the 10.0 vol % Al_2O_3-doped hafnia, although a few larger-than-average grains are seen. Surprisingly, however, abnormal grain growth is evident when it is sintered at 1600 °C for more than 4 h. The abnormal grain growth of the hafnia matrix led to an elongated or angular grain morphology.

As shown in Fig. 7a–c, the three compositions are different in grain-size distributions of both the hafnia

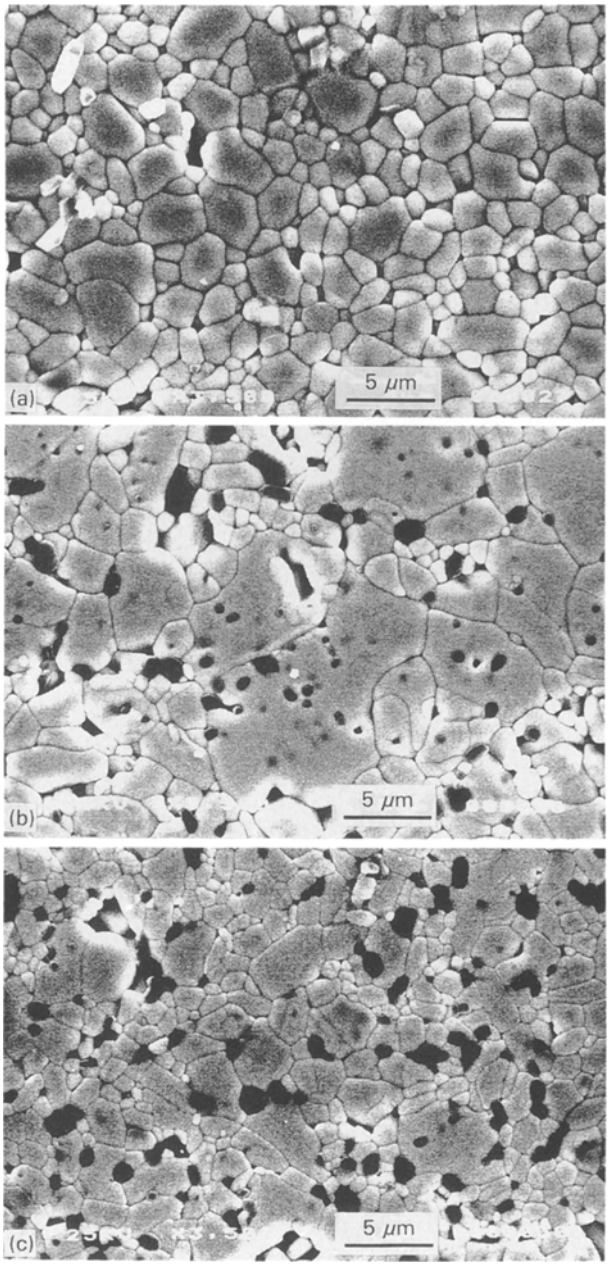

Figure 5 Scanning electron micrographs showing the polished surfaces of the hafnias containing (a) 0 (b) 5 and (c) 10 vol % Al_2O_3, respectively, which were sintered at 1600 °C for 2 h.

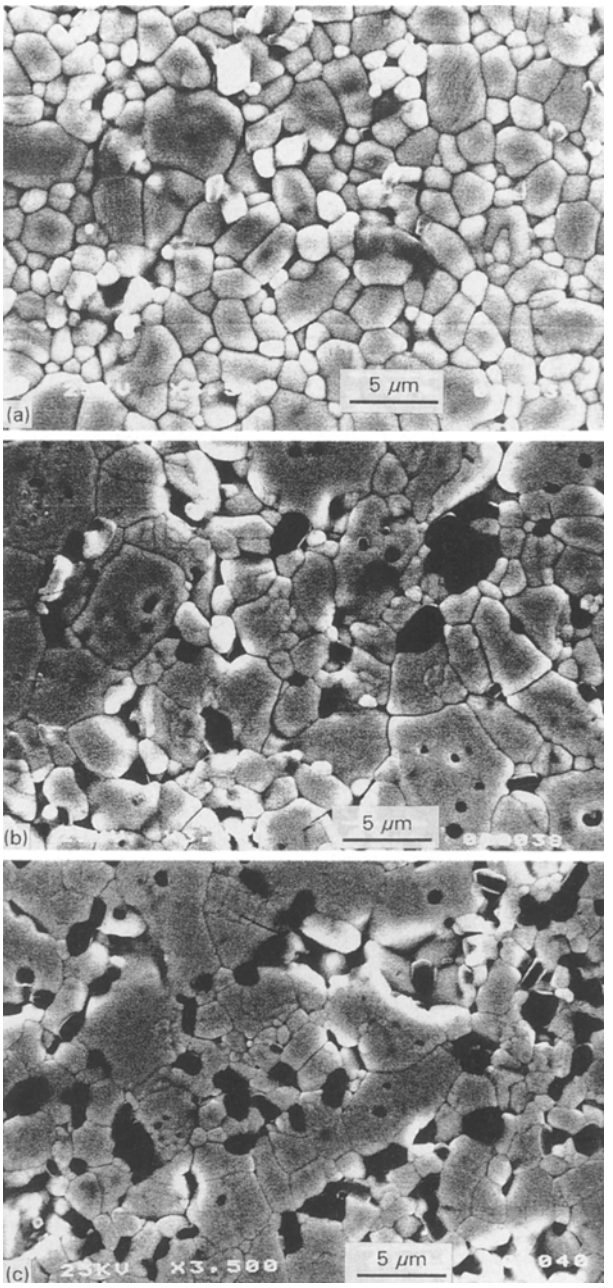

Figure 6 Scanning electron micrographs showing the polished surfaces of the hafnia containing (a) 0, (b) 5 and (c) 10 vol % Al_2O_3, respectively, which were sintered at 1600 °C for 12 h.

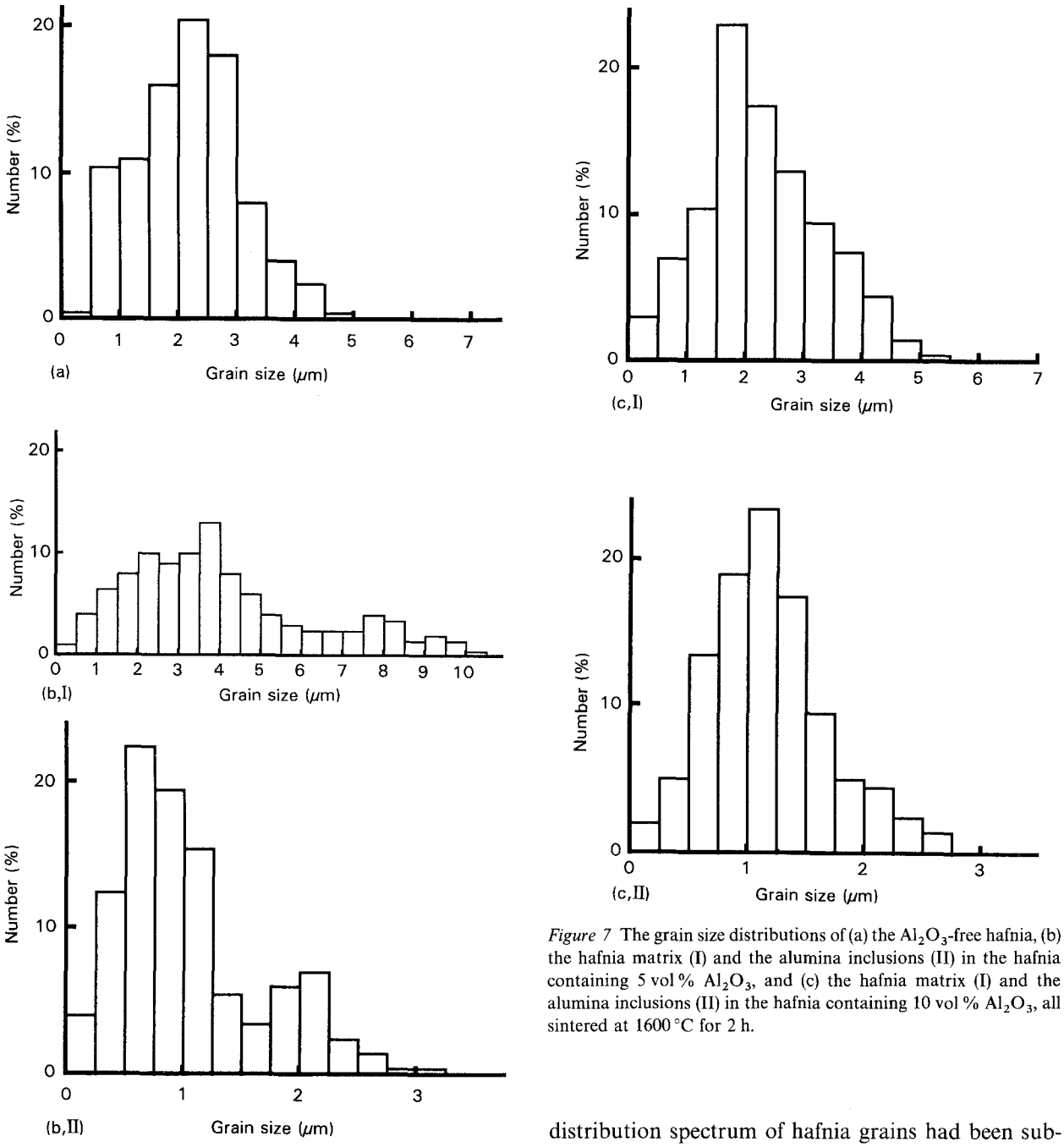

Figure 7 The grain size distributions of (a) the Al_2O_3-free hafnia, (b) the hafnia matrix (I) and the alumina inclusions (II) in the hafnia containing 5 vol % Al_2O_3, and (c) the hafnia matrix (I) and the alumina inclusions (II) in the hafnia containing 10 vol % Al_2O_3, all sintered at 1600 °C for 2 h.

matrix and the alumina inclusions when sintered at 1600 °C for 2 h. The hafnia grains in the composition which contains 5.0 vol % Al_2O_3 are distributed on the widest spectrum from less than 0.5 μm up to more than 10 μm. In contrast, the grain-size distribution in the Al_2O_3-free hafnia is the narrowest one of the three compositions. The alumina inclusions in the former exhibit a bimodel-like size distribution. As shown in Fig. 5b, the relatively smaller alumina inclusions are situated within the large hafnia grains and those relatively larger ones at the grain boundaries and grain junctions of the hafnia matrix. It was observed that an increase in sintering time at 1600 °C led to a widening in the grain-size distribution in all three compositions. Fig. 8a–c show the grain-size distributions for the compositions sintered at 1600 °C for 12 h, containing 0.0, 5.0 and 10.0 vol % Al_2O_3, respectively. In comparison with those shown in Fig. 7a–c, the size distribution spectrum of hafnia grains had been substantially widened in the composition containing 10.0 vol % Al_2O_3.

To discuss the effect of an alumina addition on the microstructural development of hafnia ceramics presented above, three parameters need to be considered: (i) the alumina addition or part of the alumina addition as a dopant in promoting grain coarsening by forming a HfO_2–Al_2O_3 solid solution, although the solubility of alumina in hafnia is low [21, 22]; (ii) grain pinning of the hafnia matrix by the alumina inclusions; (iii) scavenger effect of the alumina inclusions for the silica/silicate impurity, which is the principal impurity and a parameter affecting the microstructural development at the sintering temperature [9, 10]. Obviously, the grain growth at the sintering temperature in the two Al_2O_3-containing hafnia ceramics is the overall result of the above three contributing parameters. Alumina exhibits limited solubility in hafnia at 1600 °C, because they are generally regarded as chemically competitive up to their melting points [23, 24]. A solubility of 0.1 mol % Al_2O_3 in HfO_2, which is

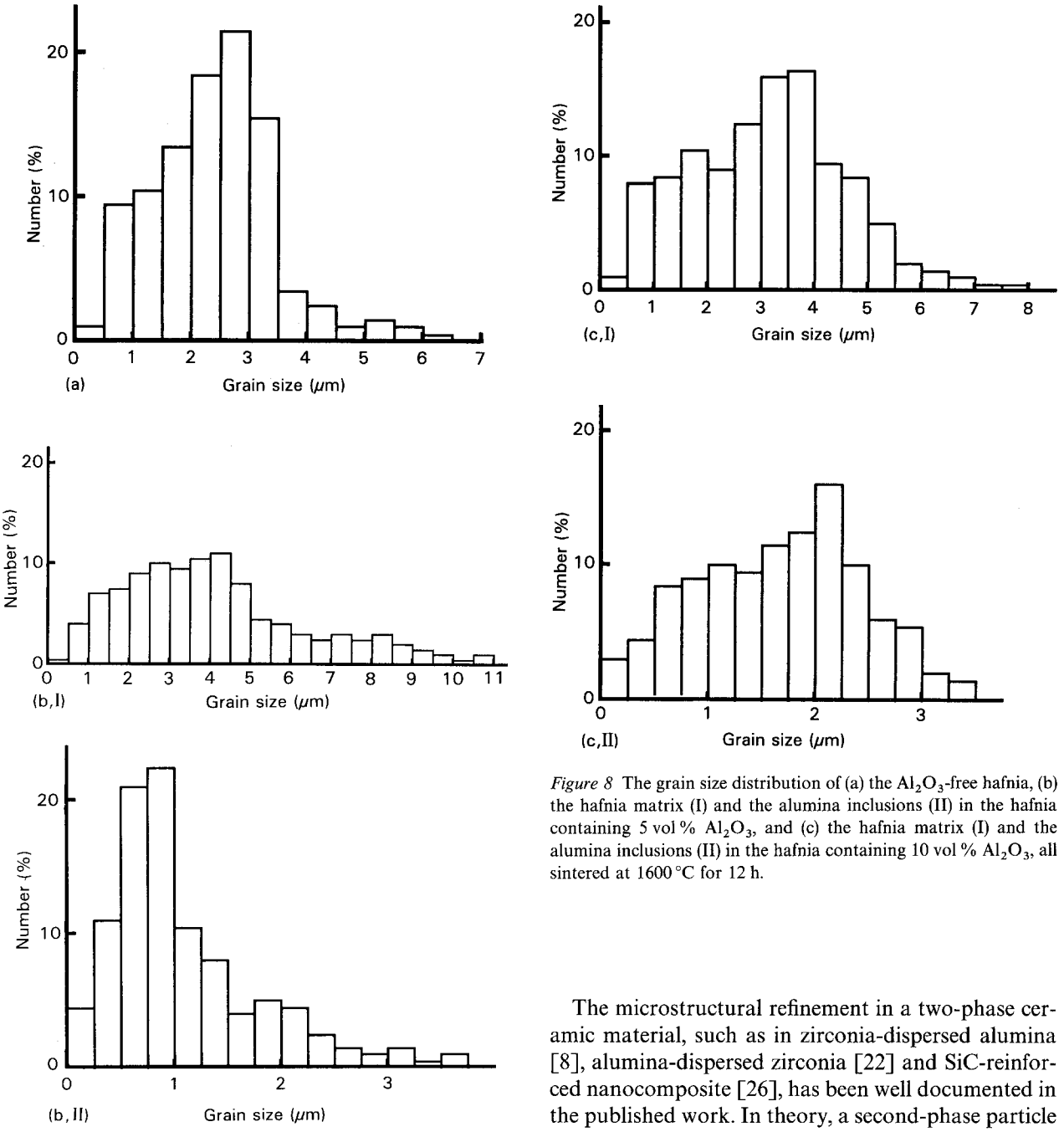

Figure 8 The grain size distribution of (a) the Al_2O_3-free hafnia, (b) the hafnia matrix (I) and the alumina inclusions (II) in the hafnia containing 5 vol % Al_2O_3, and (c) the hafnia matrix (I) and the alumina inclusions (II) in the hafnia containing 10 vol % Al_2O_3, all sintered at 1600 °C for 12 h.

analogous to that in the ZrO_2–Al_2O_3 system [9], may be quoted. To assess the effect of the limited number of Al^{3+} ions as substitutes for Hf^{4+} ions in the lattice on the microstructural development, hafnias containing 0.1 and 0.2 mol % Al_2O_3, respectively, were prepared using aluminium nitrate as the alumina source. The two materials exhibited a very similar microstructure to that of the Al_2O_3-free hafnia, and abnormal grain growth was not observed when sintered at 1600 °C. This is consistent with the experimental result that a small Al_2O_3 addition, which resulted in limited substitution of Zr^{4+} ions by Al^{3+} ions (< 0.1 mol %) in the lattice, assisted the sintering of zirconia ceramics [25]. It may, therefore, be concluded that the abnormal grain growth in the two Al_2O_3-containing hafnias is not a consequence of the limited substitution of Hf^{4+} ions by Al^{3+} ions by forming a HfO_2–Al_2O_3 solid solution.

The microstructural refinement in a two-phase ceramic material, such as in zirconia-dispersed alumina [8], alumina-dispersed zirconia [22] and SiC-reinforced nanocomposite [26], has been well documented in the published work. In theory, a second-phase particle at the grain boundary or grain junction of a ceramic matrix will exert a dragging force to the mobile grain boundary and therefore slow it down at the sintering temperature [21]. Both the size and volume fraction of the second phase were shown to be important in determining the total dragging effect applied by the second phase to the mobile grain boundaries. In zirconia-dispersed alumina ceramics, for example, a volume fraction of 5.0 vol % ZrO_2 was suggested by Lange and Hirlinger [27] as the minimum amount of zirconia addition in order to achieve an effective refinement in microstructural development. This was believed to result in the occurrence of at least one zirconia inclusion at each triple grain junction, Obviously, the total number of zirconia inclusions is dependent on their particle size for a given volume fraction. Therefore, Hori *et al.* [28] achieved an effective grain pinning in the zirconia-dispersed alumina when 2.5 vol % ultra-fine zirconia particles (0.26 μm) were dispersed in an alumina matrix. It may be assumed that the same pinning effect occurs in the

hafnia–alumina two-phase ceramics because hafnia is almost identical to zirconia in both the crystal structure and the reactivity with alumina [2]. In terms of an increased number of the second-phase alumina particles, there are more hafnia grains being pinned in the composition containing 10 vol % Al_2O_3 than in the composition containing 5.0 vol % Al_2O_3. This may explain the fact that the average hafnia grain size of the former is smaller than that of the latter. As shown in Figs 3 and 4, however, the average grain size of the hafnia matrix containing 5.0 vol % Al_2O_3 is almost double that of the Al_2O_3-free hafnia. Furthermore, the average grain size of the hafnia matrix containing 10.0 vol % Al_2O_3 is larger than that of the Al_2O_3-free composition when sintered at 1600 °C for more than 8 h. All these experimental results suggest that the alumina addition promoted the grain growth of the hafnia matrix at the sintering temperature. It is thus apparently wrong to assume that the grain pinning is the only consequence when the alumina particles are retained in the hafnia matrix as second-phase inclusions.

Hafnia and zirconia are originally processed from either hafnium-containing zircon ($ZrSiO_4$) or silicate-contaminated baddeleyite [2, 11]. An amorphous silica/silicate was observed to occur as a grain-boundary phase in most of the zirconia-based ceramics such as in tetragonal zirconia polycrystals (TZP) and fully stabilized cubic zirconia [13, 14, 16]. The presence of such a silicon-rich liquid phase at the sintering temperature resulted in the formation of a rounded grain morphology. As will be discussed below, there exists a continuous silicon-rich layer phase at the grain boundaries in the Al_2O_3-free hafnia, indicating that silica (0.1–0.2 wt %) is the principal impurity in the as-received hafnia powder used in the present work. Therefore, liquid-phase sintering is one of the important features for the Al_2O_3-free hafnia at the sintering temperature. Any silica/silicate impurity will be dissociated from the hafnia when the sintering temperature is above the dissociation temperature of hafnium silicate at around 1540 °C [29]. A silicon-rich liquid phase, which wets the hafnia grains, will be present at the grain boundaries and grain junctions at the sintering temperature. Firstly, certain powder agglomerates, which tend to result in an exaggerated grain growth and differential sintering, may be dispersed as a result of the penetration by the wetting liquid phase [30]. Secondly the grain-boundary segregant layer may act as a barrier for any mass transport from one grain to a neighbouring grain if the solubility and diffusivity of the solid in the liquid phase are low [14, 16]. Fig. 9a–d are four bright-field transmission electron micrographs showing the microstructure of a few selected grain boundaries and grain junctions in the Al_2O_3-free hafnia sintered at 1600 °C for 2 h. It is seen that there exists an amorphous pocket phase at the majority of the triple grain junctions and a continuous amorphous layer at the grain boundaries. The hafnia grains exhibit a rounded morphology at the triple grain junctions wherever there exists an amorphous phase at the pocket. The thickness of the segregant layer varies in the range of < 1.0 up to 10.0 nm. The amorphous nature of the grain-boundary phases was clearly shown by the ring-like selected-area diffraction (SAD) patterns. Energy-disperse X-ray (EDX) analysis indicated that these amorphous phases were silicon-rich in composition, with small amounts of aluminium and hafnium (both less than 15 at %) being present. It was estimated that 0.1–0.2 wt % SiO_2 existed in the starting hafnia powder, resulting in the formation of these silicon-rich grain-boundary phases at the sintering temperature. To study the overall solubility of hafnia in the silicon-rich grain-boundary phase, more than 30 EDX spectra were obtained from the amorphous phases of various sizes and shapes and were compared for the intensity of hafnium count. It was revealed that the intensity decreased with increasing size of the pocket phase. This implies that part of the X-ray count for hafnium is from the bulk hafnia grains. It may be concluded, by taking into account the fact that the total estimated amount of hafnium from the spectrum with the highest hafnium count is less than 15 at %, that hafnia exhibits a low solubility in the silicon-rich liquid phase at the sintering temperature. This is very similar to the solubility of zirconia in a silicon- and aluminium-rich grain-boundary phase in the tetragonal zirconia polycystalline ceramics [14]. These TEM studies support the considerations discussed above: (i) the silicon-rich liquid phase wets hafnia grains and penetrates through the grain boundaries; (ii) hafnia exhibits a low solubility in the silicon-rich amorphous phase, which therefore acts as a segregant layer at the grain boundaries. Both of these factors are helpful in inhibiting grain growth in the undoped hafnia ceramic at the sintering temperature.

Fig. 10a–d shows four bright-field transmission electron micrographs showing examples of the alumina inclusions entrapped at either a grain boundary or a grain junction of the hafnia matrix in the composition containing 5.0 vol % Al_2O_3, sintered at 1600 °C for 2 h. The alumina grains appeared to be brighter than the hafnia grains under the transmitted electron beam due to the lower atomic number of aluminium. These alumina grains are generally larger in size and more angular in morphologies than those entrapped inside hafnia grains. There exists an electron-transparent cusp area, the morphology of which is irregular and lies along the adjacent grain boundaries, at most of the Al_2O_3–HfO_2 (or Al_2O_3)–HfO_2 triple grain junctions. The size of the cusp areas varies from < 10 nm up to 350 nm. Selected-area electron diffraction analysis indicated that they were amorphous and EDX compositional analysis showed that they were silicon-rich in composition with limited amounts of aluminium and hafnium being present. The overall aluminium content in the amorphous pocket phases (20.7 at %) in the 5.0 vol % Al_2O_3-doped hafnia was slightly higher than that in the pocket phases of the Al_2O_3-free hafnia ceramic discussed above (12.4 at %), when 20 EDX spectra were analysed and compared between the two materials. The overall hafnium content in the amorphous phases found in the hafnia ceramic doped with 5.0 vol % Al_2O_3 (6.9 at %), is slightly lower than that in the

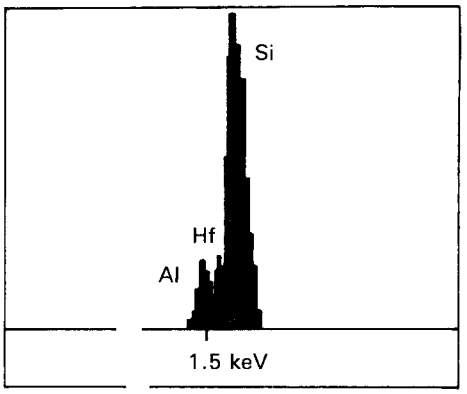

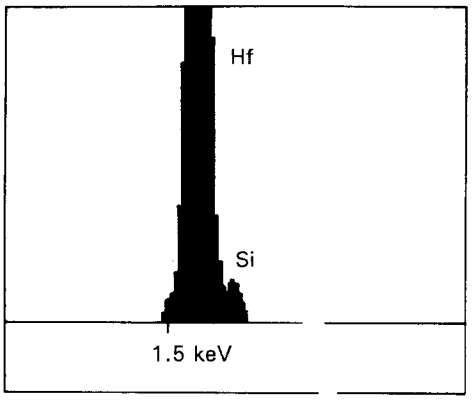

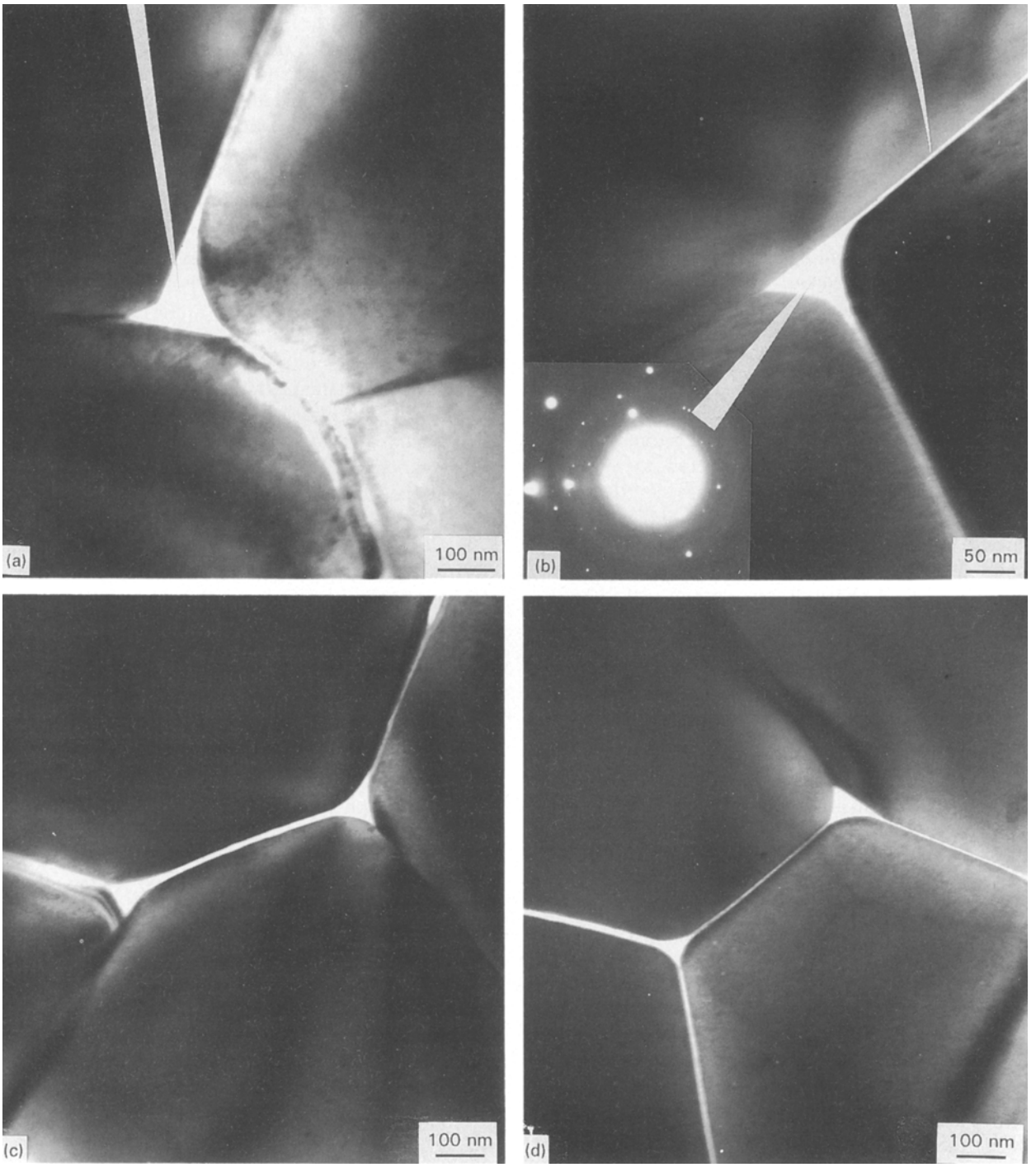

Figure 9 (a–d) Four bright-field transmission electron micrographs showing the microstructure of the Al_2O_3-free hafnia sintered at 1600 °C for 2 h. Amorphous phases, which are silicon-rich, are observed to occur at the grain boundaries and grain junctions.

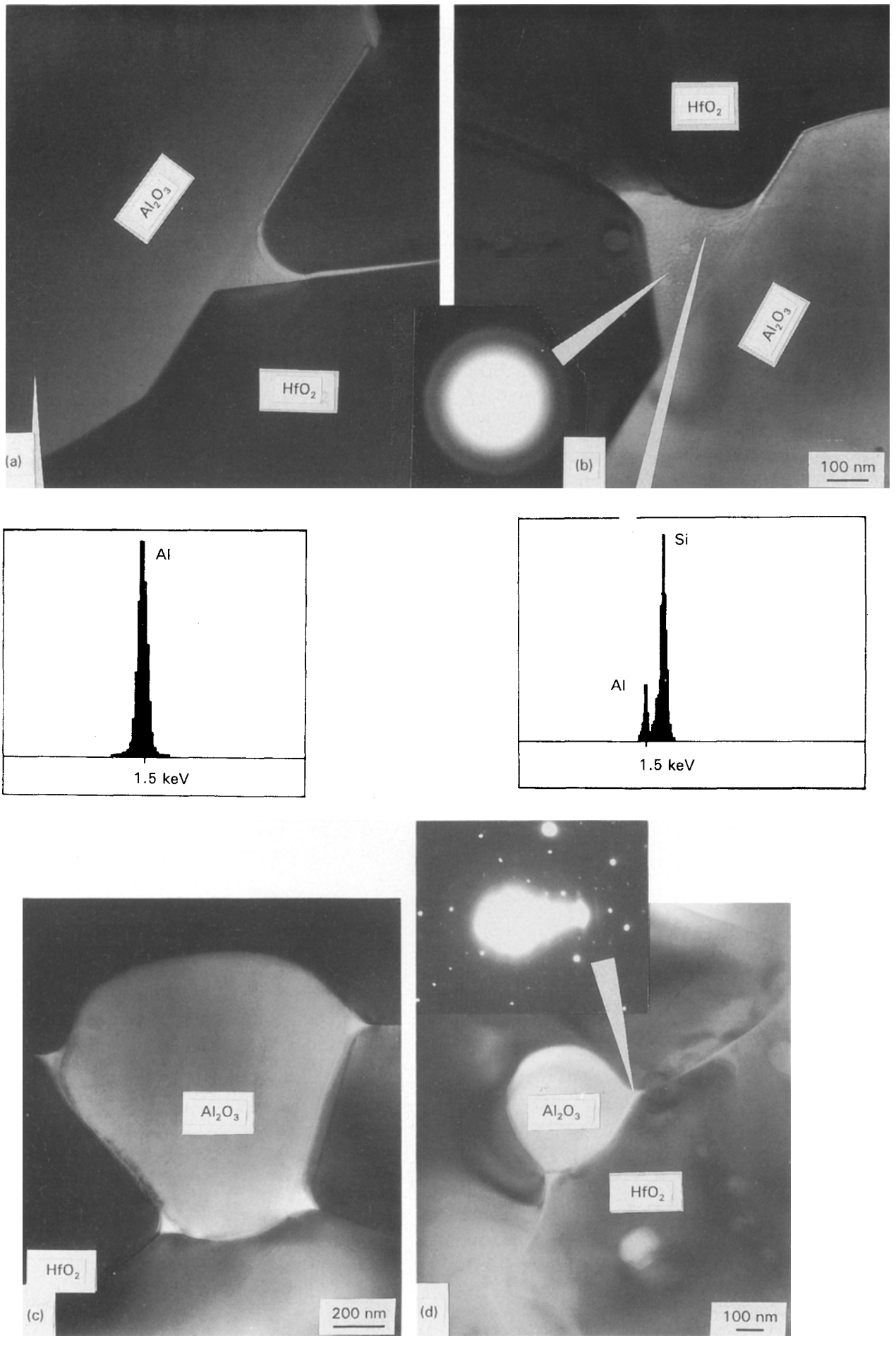

Figure 10 (a–d) Four bright-field transmission electron micrographs showing examples of the alumina inclusions entrapped at either a grain boundary or a grain junction in the hafnia containing 5 vol % Al_2O_3, which was sintered at 1600 °C for 2 h.

undoped hafnia ceramic (10.1 at %), when EDX spectra from more than 20 pocket phases were compared. The intensity of the hafnium count decreases with increasing size of the pocket phase. This implies that part of the X-ray count for hafnium in the spectra for the small pocket phases is from the bulk hafnia grains and the solubility of hafnia in the silicon-rich liquid phase at the grain boundaries is low. Fig. 11 is a bright-field transmission electron micrograph showing an Al_2O_3 grain entrapped within a large hafnia grain, together with an EDX spectrum for the amorphous cusp at the alumina–hafnia interface. The same as many other small Al_2O_3 inclusions entrapped within hafnia grains, it exhibits a rounded morphology. One or two cusp areas, which are electron transparent, were found at the interface between each alumina inclusion and the hafnia matrix grain. EDX phase analysis showed that these amorphous cusps are rich in silicon, with noticeable amounts of aluminium and hafnium being present. In comparison with the glassy phases concentrated at the Al_2O_3–HfO_2 (or Al_2O_3)–HfO_2 triple grain junctions, they exhibited a slightly higher aluminium content (up to 30 at %). As has been established, the occurrence of an intragranularly positioned second-phase particle in a two-phase ceramic system is a consequence of the break-away of an impeded mobile grain boundary from the second-phase particle at the sintering temperature [27]. The intragranularly positioned alumina particle was therefore initially at a grain boundary or a triple grain junction of the hafnia matrix. As will be discussed later, alumina grains have a great affinity for the silicon-rich liquid phases at the sintering temperature and accumulate them from the grain boundaries, forming amorphous cusp areas at the Al_2O_3–HfO_2 (or Al_2O_3)–HfO_2 tripe grain junctions. The same as any other alumina grains entrapped at the grain boundaries or grain junctions, the intragranularly positioned Al_2O_3 particle accumulated the silicon-rich solute phase from the grain boundaries prior to being swallowed up by the growing hafnia grains.

The most striking difference between the Al_2O_3-free and Al_2O_3-doped hafnia ceramics discussed above is the size (average of the three heights for each triangular boundary phase) distribution of silicon-rich amorphous phases at the grain junctions, when 100 pocket phases from a specific area in each material were analysed and compared. Fig. 12a and b show the size distribution of the amorphous pocket phases in the Al_2O_3-free and 5.0 vol % Al_2O_3-doped hafnias, respectively, sintered at 1600 °C for 2 h. The majority of the pocket phases in the undoped hafnia lies within a spectrum of 10–150 nm, with the average size being 67 nm. In comparison, the pocket phases in the 5.0 vol % Al_2O_3-doped hafnia are distributed over a much wider spectrum, ranging from 10–350 nm. It was also noted that more than 90% of those > 100 nm pocket phases occurred at the triple grain

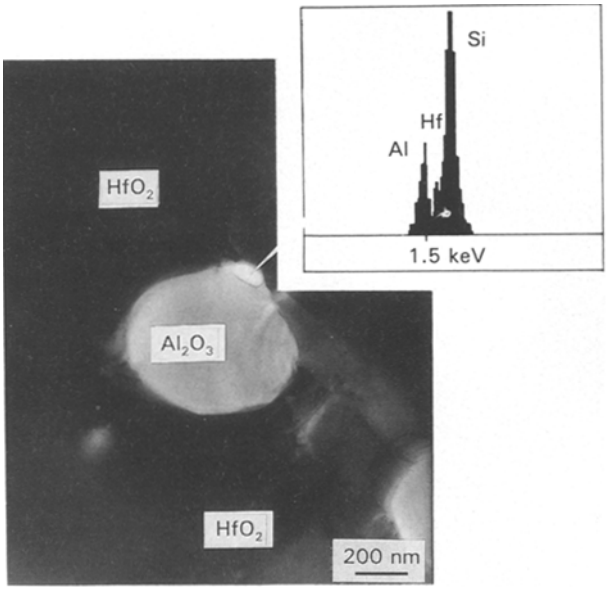

Figure 11 A bright-field transmission electron micrograph showing an Al_2O_3 grain entrapped within a large hafnia grain in the HfO_2–5 vol % Al_2O_3 sintered at 1600 °C for 2 h. There is an amorphous cusp, which is silicon-rich as indicated by the EDX spectrum, at the alumina–hafnia interface.

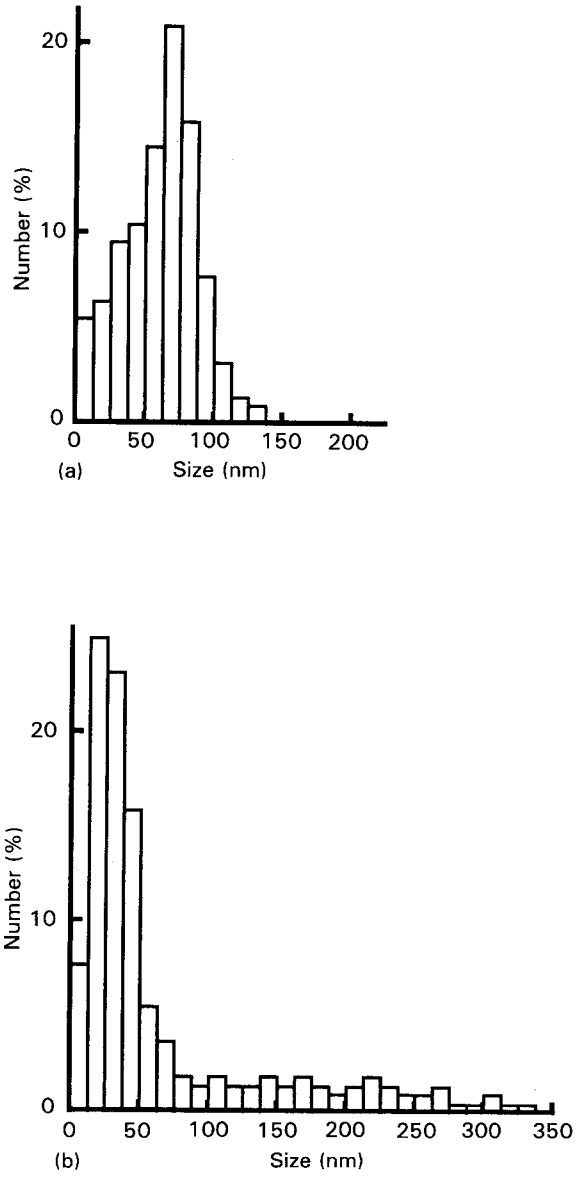

Figure 12 The size distribution of the amorphous pocket phases in (a) the Al_2O_3–free and (b) 5 vol % Al_2O_3-doped hafnias, which were sintered at 1600 °C for 2 h.

junctions involving at least one alumina grain. The average thickness of the amorphous segregant layers at the grain boundaries in the 5.0 vol % Al_2O_3 doped hafnia is 1.7 nm, compared with an average layer thickness of 5.2 nm in the Al_2O_3-free hafnia ceramic when 80 boundary segregant layers from a specific region in each material were analysed. Furthermore, the continuous nature of the segregant layers was damaged by the presence of Al_2O_3 particles in the former. For example, 17 of the 80 grain boundaries studied in the Al_2O_3-doped hafina showed no such grain-boundary segregant layer. This was contrasted to the fact that no "clean" grain boundaries were found amongst the 80 grain boundaries counted in the Al_2O_3-free hafnia ceramic. All these statistical data suggested that the presence of the 5.0 vol % Al_2O_3 grains in the hafnia matrix led to less-uniform distribution of the silicon-rich amorphous phases at the grain boundaries and grain junctions in the Al_2O_3-doped hafnia than in the Al_2O_3-free hafnia. The amorphous phase is largely concentrated at the triple grain junctions involving an alumina grain. It is thus obvious that the alumina grains accumulated the silicon-rich grain-boundary phase at the sintering temperature.

As mentioned earlier, the effect of an alumina addition as a scavenger for the silica/silicate impurity in zirconia ceramics has been demonstrated by both ionic conductivity measurement and microstructural study carried out using analytical transmission electron microscopy [9, 10]. The ionic conductivity of both fully stabilized and partially stabilized zirconia ceramics is improved when an appropriate amount of alumina is introduced as a grain-boundary phase. Ionic conductivity of a polycrystalline ceramic material is determined by a combination of the conductivity of the grain phases and that of grain-boundary phases, if present [31]. The presence of a grain-boundary phase of low ionic conductivity will apparently lead to a decrease in the overall ionic conductivity of a polycrystalline material. Zirconia raw materials tend to be contaminated by a level of silica or silicate impurity. A silicon-rich glassy phase, which is a poor ionic conductor, is likely to occur in zirconia ceramics as a grain-boundary phase. Accordingly, a polycrystalline zirconia ceramic exhibits a lower ionic conductivity than a zirconia single crystal of the same composition. The presence of a volume fraction of alumina grains, which are chemically competitive to zirconia, at the grain boundaries and grain junctions does not alter the intrinsic electrical properties of the zirconia grains. Furthermore, the alumina grains themselves are not ionically conductive. The improvement in the overall ionic conductivity was therefore considered to be due to a decrease in the resistance caused by the silicon-rich glassy phase present at the grain boundaries. It has been suggested that the alumina grains act as a scavenger for the silicon-rich boundary phases at the sintering temperature, as they have a great affinity for SiO_2 [10]. It was observed using high-resolution transmission electron microscopy that there existed a well-defined amorphous phase at the grain boundaries and grain junctions in the Al_2O_3-free zirconia ceramics, which exhibited a rounded grain morphology at the triple grain junctions [13, 14]. The amorphous phases are silicon-rich, with trace levels of other commonly observed impurity elements in oxide ceramics being present, as indicated by the EDX analysis equipped to the TEM. In contrast, the intergranular glassy phase was less-frequently observed to occur in the Al_2O_3-doped zirconia ceramics. The alumina addition has therefore resulted in a "clean-up" of the silicon-rich glassy phase present at the grain boundaries and grain junctions in zirconia ceramics. In a microstructural study of the sintered ionically conductive zirconia ceramics doped with an alumina addition using analytical TEM, Butler and Drennan [10] observed that the alumina grains at the zirconia grain boundaries and grain junctions were frequently associated with electron-transparent cusp areas rich in silicon and aluminium. Furthermore, small inclusions, which are rich in silicon or/and zirconium, of varying electron opacity and size were observed to occur within the alumina grains.

Thermodynamically, Al_2O_3 has a greater affinity for SiO_2 than does ZrO_2 at temperatures above 1540 °C. As pointed out by Anseau *et al.* [29], 1540 °C is the highest temperature at which zirconia and silica combine to yield zircon ($ZrSiO_4$). The same temperature may be regarded as the dissociation temperature for $ZrSiO_4$. It is therefore thermodynamically unfavourable for the zirconia grains to react with the silicon-rich grain-boundary phase at 1600 °C [32]. In comparison, Al_2O_3 has a great potential to react with SiO_2, forming thermodynamically stable crystalline mullite-type phases at temperatures as low as 980 °C [33]. The reaction $3Al_2O_3 + 2SiO_2 = Al_6Si_2O_{13}$ has a free-energy change of -5.8 kcal at 1422 °C [34, 35]. An activity of 0.03 was estimated by Butler and Drennan [10] for silica at 1600 °C while second-phase particles of alumina are present. At temperatures above 1540 °C, the presence of alumina promotes the dissociation of zircon as the reaction $2ZrSiO_4 + 3Al_2O_3 = 2ZrO_2 + 2SiO_23Al_2O_3$ has a more negative free energy change than the reaction $ZrSiO_4 = ZrO_2 + SiO_2$ [36]. Therefore, alumina grains will have an even greater affinity for the silica impurity when it occurs as a zirconium silicate than as a free silica in the starting powder. All these thermodynamic data suggest that the alumina grains will accumulate the silica/silicate impurity from the grain boundaries and grain junctions in the Al_2O_3-doped zirconia ceramics. It was proposed that the alumina grains accumulated the silicon-rich grain-boundary solute phase by the following mechanism [10]: at the sintering temperature, densification and grain growth involve various grain boundaries moving towards their centres of curvature. The motion of a moving grain boundary, which is dragged by a segregant solute layer and exhibits a lowered mobility, will be impeded on meeting an immobile alumina particle [15]. Solute transfer via rapid boundary diffusion to the alumina particle will occur as soon as it intersects the grain boundary, creating two silicon-rich cusps at the Al_2O_3–ZrO_2–ZrO_2 triple grain junctions. The solute transfer and possible chemical reactions at the

Al_2O_3 interface continue until the solute drag force on the boundary has been reduced by an amount equal to the maximum drag force of the Al_2O_3 particle. Breakaway of the grain boundary from the Al_2O_3 particle and the accumulated solute phases then takes place, creating a cleaned grain boundary.

On considering the fact that hafnia is almost identical to zirconia in both crystal structure and reactivity [2], it is believed that the scavenger effect discussed above is equally applicable to hafnia ceramics. This is supported by the experimental results shown in Figs 10a–d and 12b, where large silicon-rich amorphous pocket phases are mainly concentrated at the triple grain junctions involving an alumina grain. It is to be concluded that the silicon-rich glassy phase at the grain boundaries and grain junctions is responsible for the refined microstructure in the Al_2O_3-free hafnia if the scavenger effect discussed above does occur in the Al_2O_3-doped hafnia compositions. For a simple verification, a high-purity hafnia (99.95% pure, Aldrich, Dorset, UK) powder compact was sintered at 1600 °C for 2 h. The sintered material exhibited an average grain size of 2.84 μm, although abnormal grain growth was not substantial. Apparently, its average grain size is larger than that of the Al_2O_3-free hafnia sintered at the same temperature and time. The increased grain size may be explained by the decreased thickness of the segregant layers (1–2 nm) observed at the grain boundaries in the high-purity hafnia. The continuous nature of the segregant layers along the grain boundaries may be helpful in explaining the fact that abnormal grain growth was not substantial in the high purity material. The effect of a liquid grain-boundary phase on the microstructural development of hafnia ceramics is not well documented in the published work. Again, an analogy may be made by looking at the impact of a silica/silicate phase, either as a powder impurity or as a deliberately introduced additive, on the microstructure and mechanical properties of zirconia-based ceramic materials [13, 14, 16]. The presence of a glassy grain-boundary phase, on the one hand, results in a degradation in the mechanical properties, such as in fracture strength and fracture toughness of tetragonal zirconia polycrystals (TZP) as the autocatalytic nature of the stress-induced transformation toughening is depressed [37]. On the other hand, the presence of an appropriate glassy phase at the grain boundaries and grain junctions improves the superplastic deformation behaviour of zirconia-based ceramics, by restraining grain growth [38]. The most important role played by a small silica addition in zirconia ceramics is in enhancing densification and refining microstructure at the sintering temperature. For example, Shackelford *et al.* [39] observed that the sintered density of a partially stabilized zirconia with either 3.5 wt % CaO or 2.0 wt % MgO increased with increasing silica content in the range 0–2 wt %. The sintering involved a liquid phase consisting of calcium or magnesium silicates, which was largely concentrated at the grain boundaries and grain junctions of the sintered zirconia ceramic. A glassy grain-boundary phase has been observed to occur in most, if not all, tetragonal zirconia polycrystals (TZP) [13–16]. The coexistence of rounded and polygonal-faceted zirconia grains is a result of the non-uniform distribution of the glassy phase at the grain boundaries and grain junctions. A minimal level of the glassy phase is found in the regions of sharply faceted grains and a considerable level is found in the regions of rounded grains. The composition of these glassy phases, which are liquid phases at the sintering temperature, is dependent on parameters such as the types and amounts of additive or impurity, stabilizer, and sintering temperature and time.

Several suggestions have been made to account for the retarded grain growth in the presence of a liquid grain-boundary phase in oxide ceramics, including a decreased grain-boundary mobility by the dragging liquid phase [15, 17] and a low solubility or diffusivity of cation ions or both in the silicon-rich grain-boundary phases [14]. The grain growth in the Al_2O_3-free and Al_2O_3-doped hafnia ceramics involves hafnium transfer across the grain-boundary segregant layer via a dissolution-and-reprecipitation mechanism at the sintering temperature. It is necessary for hafnia to have both a high solubility and a diffusivity in the segregant layer phase for a fast grain growth. As discussed above, hafnia exhibits limited solubility in the boundary phase and therefore a slow grain-growth rate is expected. This agrees well with the fact that zirconia exhibits a low solubility in many segregant layer phases of differing compositions, as indicated by the experimental results obtained by several research groups [14, 16, 40]. The materials studied by these independent institutions were different in composition and type and amount of the grain-boundary impurities. However, a low zirconia solubility was found in the glassy grain-boundary phase in each of the materials investigated. Grain growth of zirconia-based ceramics is also limited by the sluggish diffusion of cation ions, such as Zr^{4+}, Y^{3+} and Ca^{2+}, in a SiO_2-based grain-boundary phase. As was shown by Stoto *et al.* [16], yttrium exhibited a very sluggish diffusion in a non-equilibrium SiO_2-based grain-boundary phase. A compositional difference in yttria content was found between both the tetragonal and tetragonal grains and the tetragonal and cubic grains in Y-PSZ. The sluggish yttrium transfer through the grain-boundary segregant layer has been suggested to be responsible for the retarded grain growth in the partially stabilized zirconia ceramics consisting of intergranular cubic and tetragonal grains. Therefore, the average grain size of the materials with composition lying in the tetragonal + cubic two-phase region is much smaller than those lying in either tetragonal or cubic single-phase region [41]. Similarly, a grain size–sintering time relation of $G = A\,t^{1/3}$ was demonstrated for a 7.5 wt % CaO-stabilized zirconia at 1520 °C, in which G is grain size, t sintering time and A is a constant [42]. There existed a glassy grain-boundary phase in this material and the grain-growth rate was therefore lowered.

As discussed earlier, the Al_2O_3-free hafnia ceramic demonstrated a smaller average grain size and narrower grain-size distribution than the Al_2O_3-doped hafnia ceramics on sintering at 1600 °C. Abnormal grain

growth was evident in the latter two materials. The average grain size of the 10.0 vol % Al_2O_3-doped material was larger than that of the Al_2O_3-free hafnia on sintering at 1600 °C for more than 8 h, although it was smaller than the average grain size of the 5.0 vol % Al_2O_3-doped composition. A relationship in average grain size of HfO_2 > HfO_2–5.0 vol% Al_2O_3 > HfO_2–10.0 vol % Al_2O_3 would be expected in terms of grain-pinning effect [27]. Therefore, grain pinning is not the dominant effect in association with the alumina addition in the silica-contaminated hafnia. As noted above, the alumina grains have a great affinity for SiO_2 and act as a scavenger for the silicon-rich impurity phase at the grain boundaries and grain junctions, creating "cleaned" grain boundaries and grain junctions. The silicon-rich glassy grain-boundary phase played a critical role in inhibiting grain growth of the Al_2O_3-free hafnia at the sintering temperature. The low solubility of hafnia in the liquid segregant layer and therefore a sluggish hafnia transfer across the grain-boundary phase are responsible for the retarded grain growth and the microstructural refinement. The high-purity (99.95%) hafnia ceramic demonstrated a larger average grain size than the Al_2O_3-free hafnia on sintering at 1600 °C for 2 h, owing to a decrease in the thickness of the boundary segregant layer. However, the continuous nature of the segregant layer prevents the occurrence of substantial abnormal grain growth. In the Al_2O_3-doped materials, however, the average thickness of the grain-boundary segregant layer was reduced and more importantly the continuous nature of the layer structure was damaged by the presence of the alumina particles. Therefore, the diffusion barrier for hafnia transfer across the grain boundaries is removed either partially or completely, depending on the amount of the residual segregant phase left at the grain boundaries and grain junctions. Rapid grain growth is expected to occur in the regions where the grain boundaries are completely "cleaned up" by the alumina additive, although grain pinning by the alumina particles may be occurring concurrently. This explains the abnormal grain growth observed in the two Al_2O_3-doped hafnia ceramics. Specifically, the scavenger effect of the alumina grains for the silicon-rich impurity dominates the microstructural development in 5.0 vol % Al_2O_3-doped hafnia at the sintering temperature. Grain pinning by the 5.0 vol % Al_2O_3 is insufficient to stop the exaggerated grain growth. The effectiveness of grain pinning increases with an increase in the Al_2O_3 content in the hafnia matrix. The increased importance of the grain pinning by the alumina particles results in a smaller average grain size in the 10.0 vol % Al_2O_3-doped hafnia than in the 5.0 vol % Al_2O_3-doped hafnia, although the continuous nature of the grain-boundary segregant layer may be further damaged by the increased alumina addition.

4. Conclusions

Abnormal grain growth occurs in alumina-doped hafnia ceramics on sintering at 1600 °C. The hafnia matrix containing 5.0 vol % Al_2O_3 exhibits an average grain size of almost double that of the Al_2O_3-free hafnia matrix, coupled with a much wider grain-size distribution. The material containing 10.0 vol % Al_2O_3 shows a smaller average grain size than the composition containing 5.0 vol % Al_2O_3. However, its average grain size is still larger than that of the Al_2O_3-free hafnia, on sintering at 1600 °C for more than 8 h. Grain growth in the Al_2O_3-free hafnia is inhibited by the presence of a silicon-rich glassy phase, in which hafnia exhibits a low solubility, at the grain boundaries and grain junctions. The Al_2O_3 particles act as a scavenger for the silicon-rich glassy phase, damaging the continuous nature of the grain-boundary segregant layer and promoting grain growth in the Al_2O_3-doped hafnia ceramics. The microstructural development at the sintering temperature is an overall result of the concurrent scavenger effect and grain pinning by the alumina particles.

Acknowledgements

The authors thank SERC for providing financial support through the IRC in Materials for High Performance Applications at the University of Birmingham.

References

1. R. C. GARVIE, R. H. HANNINK and R. T. PASCOE, *Nature (Lond.)* **258** (1975) 703.
2. J. WANG, H. P. LI and R. STEVENS, *J. Mater. Sci.* **27** (1992) 5397.
3. R. RUH and W. R. CORFIELD, *J. Am. Ceram. Soc.* **53** (1970) 126.
4. H. J. GARRETT, *Am. Ceram. Soc. Bull.* **42** (1963) 201.
5. J. WANG and R. STEVENS, *Ceram. Acta.* **3** (1991) 41.
6. S. L. DOLE, O. HUNTER Jr and F. W. CALDERWOOD, *J. Am. Ceram. Soc.* **63** (1980) 136.
7. S. L. DOLE, O. HUNTER Jr and C. J. WOOGE, *ibid.* **60** (1977) 488.
8. F. F. LANGE, *J. Mater. Sci.* **17** (1982) 225.
9. H. BERNARD, Report CEA-R-5090. Commissariat a l'Energie Atomique, CEN-Saclay, France (1981).
10. E. P. BUTLER and J. DRENNAN, *J. Am. Ceram. Soc.* **65** (1982) 474.
11. R. STEVENS, "An introduction to zirconia" (Magnesium Elektron, Twickenham, UK, 1986).
12. C. E. CURTIS and H. G. SOWMAN, *J. Am. Ceram. Soc.* **36** (1953) 190.
13. M. RUHLE, N. CLAUSSEN and A. H. HEUER, in "Advances in Ceramics," Vol. 12, "Science and technology of zirconia II", edited by N. Claussen, M. Ruhle and A. H. Heuer (American Ceramic Society, Columbus, OH, 1984 pp. 352–70.
14. H. SCHUBERT, N. CLAUSSEN and M. RUHLE, *ibid.* p. 766–773.
15. A. J. A. WINNUBST, G. S. A. THEUNISSEN, W. F. M. GROOT ZEVERT and A. J. BURGGRAAF, in "Science of ceramics," Vol. 14, edited by D. Taylor (Institute of Ceramics, Stoke-on-Trent, UK, 1988) pp. 309–14.
16. T. STOTO, M. NAUER and C. CARRY, *J. Am. Ceram. Soc.* **74** (1991) 2615.
17. K. KEIZER, M. J. VERKERK and A. J. BURGGAAF, *Ceram. Int.* **5** (1979) 143.
18. R. W. RICE, S. W. FREIMAN and P. F. BECHER, *J. Am. Ceram. Soc.* **64** (1981) 345.
19. R. W. RICE and S. W. FREIMAN, *ibid.* **64** (1981) 350.
20. R. W. DAVIDGE, *Acta Metall.* **29** (1981) 1695.
21. F. A. NICHOLS, *J. Appl. Phys.* **37** (1966) 4599.
22. F. F. LANGE and M. M. HIRLINGER, *J. Am. Ceram. Soc.* **70** (1987) 827.

23. A. V. SHEVCHENKO, L. M. LOPATO and G. I. GERASIMYUK, *Izv. Akad. Nauk, SSSR. Neorg. Mat.* **26** (1990) 839.
24. S. G. POPOV, M. V. PAROMOVA and Z. YA KULIKOVA, *ibid.* **26** (1990) 1002.
25. K. C. RADFORD and R. J. BRATTON, *J. Mater. Sci.* **14** (1979) 59.
26. K. NIIHARA, *J. Ceram. Soc. Jpn* **99** (1991) 945.
27. F. F. LANGE and M. M. HIRLINGER, *J. Am. Ceram. Soc.* **67** (1984) 164.
28. S. HORI, R. KURITA, M. YOSHIMURA and S. SOMIYA, in "Advances in Ceramics, Vol. 24A, "Science and technology of zirconia III", edited by S. Somiya, N. Yamamoto and H. Hanagida (American Ceramics Society, Westerville, OH, 1988) pp. 423–9.
29. M. R. ANSEAU, J. P. BILOQUE and P. FIERENS, *J. Mater. Sci.* **11** (1976) 578.
30. J. S. REED, "Introduction to the principles of ceramic processing" (Wiley, Singapore, 1989).
31. N. M. BEEKMANS and L. HEYNE, *Electrochim. Acta* **21** (1976) 303.
32. A. J. G. ELLISON and A. NAVROTSKY, *J. Am. Ceram. Soc.* **75** (1992) 1430.
33. I. A. AKSAY, D. M. DABBS and M. SARIKAYA, *ibid.* **74** (1991) 2343.
34. R. F. DAVIS and J. A. PASK, in "High temperature oxides", Part IV, "Refractory glasses, glass-ceramics and ceramics," edited by A. M. Alper (Academic Press, New York, 1970) pp. 37–76.
35. R. R. DAYAL, R. E. JOHNSON and A. MUAN, *J. Am. Ceram. Soc.* **50** (1967) 537.
36. E. DI RUPO and M. R. ANSEAU, *J. Mater. Sci.* **15** (1980) 114.
37. M. L. MECARTNEY, *J. Am. Ceram. Soc.* **70** (1987) 54.
38. Y. YOSHIZAWA and T. SAKUMA, *ibid.* **73** (1990) 3069.
39. J. F. SHACKELFORD, P. S. NICHOLSON and W. W. SMELTZER, *Am. Ceram. Soc. Bull.* **53** (1974) 865.
40. R. CHAIM, A. H., HEUER and D. G. BRANDON, *J. Am. Ceram. Soc.* **69** (1986) 243.
41. F. F. LANGE, *ibid.* **69** (1986) 240.
42. S. DOU, P. D. PACEY, C. R. MASSON and B. R. MARPLE, *ibid.* **68** (1985) C-80.

Received 3 February
and accepted 16 February 1994